although the overall pathway is different, similar regioselectivity appears with the iron analogue. Parallel with the chromium analogues and with the reaction of **2** with alkenes,[13] the less substituted end of the alkyne is coupled with the alkylidene carbon.

New isomers appear upon heating of the pyrone–iron complexes. For example, at 90 °C in THF, **5a** slowly rearranges into an isomer with identical melting point, similar ^{1}H NMR spectra, and nearly identical ^{13}C NMR spectra.[9] The new isomer was easily separated by analytical HPLC and conventional TLC and shown to have structure **6a** by X-ray diffraction.[11] Although decomposition becomes significant at long reaction times (10 h at 100 °C), the equilibrium constant can be estimated to be 3.0 at 91 ± 0.5 °C. At this temperature, the forward unimolecular rate constant is 5.4×10^{-4} min^{-1}, while the reverse rate constant is 1.8×10^{-4} min^{-1}. Heating of **6a** at 100 °C for 8.5 h also leads to a mixture from which **5a** and **6a** can be isolated, in yields of 26% and 58%, respectively. Complex **5c** shows the same behavior, producing **6c** (48% yield) and recovered **5c** (37%).

The mechanism of formation of pyrones **5** has not been established. However, a pathway can be outlined (Scheme II) which accounts for the known facts. The key ferracyclobutene intermediate **1** is suggested to undergo migratory insertion of CO (to give **7**) and α-elimination of ethoxy (to **8**). Then CO migration to the alkylidene carbon (to give **9**) and reductive elimination of EtOCO– lead to a coordinated ketene (**10**, **11**) which can assume the bonding arrangement in **12**, an obvious precursor of pyrone **5**. Intermediates related to **7** are known for iron[14] and have been postulated in the analogous alkylidene–chromium reactions,[5] although no stable example with an α-ethoxy group has been reported.

By careful monitoring of the reaction of **2** with excess 2-butyne in the absence of CO (20 °C, CH_2Cl_2, argon, 24 h), a persistent intermediate was detected. Rapid chromatography (silica gel, argon blanket) gave two products, **5a** and a brown oil, which solidified to a yellow amorphous solid at −10° C. Repeated precipitation from pentane at low temperature produced material (28% yield) which was >95% pure (^{13}C NMR) and showed spectral data compatible with structure **1a**.[15] It was unstable,

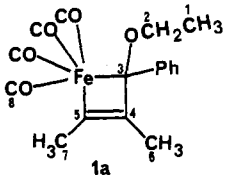

1a

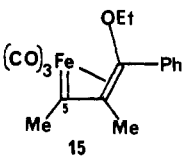

15

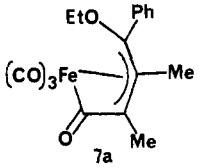

7a

decomposing to **5a** and other products at 25 °C, and proceeded to **5a** quantitatively when heated at 70 °C under CO at 55 psi. Additional data are necessary to establish the structure with certainty, but alternate bonding modes[15] such as in **15** seems unlikely, since the alkylidene carbon in **15** (C-5) would be expected at very low field (below δ 300).[16] The alternate structure **7a** is also consistent with the data, except it would be expected to show a signal in the ^{13}C NMR spectrum for the acyl carbonyl group; none is observed. Work is in progress to characterize fully a suitable derivative of **1**.

Acknowledgment. We are pleased to acknowledge support of this work through a research grant from the National Institutes of Health (GM 31352).

Supplementary Material Available: General experimental procedures, characterization data on the pyrone complexes, spectra for **1a**, and listings of atomic coordinates and details of the X-ray analyses (27 pages). Ordering information is given on any current masthead page.

(12) For additional examples of regioselectivity involving the chromium–alkylidene complexes, see: Wulff, W. D.; Tang, T. C.; McCallum, J. S. *J. Am. Chem. Soc.* **1981**, *103*, 7677–7678.

(13) Semmelhack, M. F.; Tamura, R. *J. Am. Chem. Soc.* **1983**, *105*, 6750–6752.

(14) For examples and leading references, see: Mitsudo, T.; Watanabe, H.; Watanabe, K.; Wantanabe, Y.; Takegami, Y. *J. Organomet. Chem.* **1981**, *214*, 87–92.

(15) The ^{1}H NMR spectrum and IR spectrum (supplementary material) were consistent but not revealing. In the ^{1}H NMR spectrum, the $-CH_2-$ unit in the EtO group shows diastereotopic protons, differing by 0.12 ppm, consistent with the presence nearby of a chiral center (C-3). ^{13}C NMR (63 MHz, 253 K, $CDCl_3$): δ 234.7, 234.4 (s, C=O); 138.3 (s, Ph ipso C); 128.6, 128 1 (d, Ph CH); 112.5 (s, C-4 or C-5); 106.7 (s, C-5 or C-4); 66.7 (t, C-2); 48.9 (s, C-3); 15.1, 13.8, 12.5 (q, C-1, C-6, C-7). The mass spectrum shows a peak of highest m/e at 328, consistent with loss of one CO from **1a** (or **7a**), or precisely the parent ion for **15**. The base peak appears at 188 [P − Fe $(CO)_4$], especially consistent with **1a**. Mass spectrum (70 eV, electron impact): m/e 328 (P − CO, 10%), 300 (P − 2CO, 10), 272 (P − 3CO, 42), 244 (P − 4CO, 56), 216 [P − Fe$(CO)_3$], 188 (P − Fe$(CO)_4$, 100]. The infrared spectrum was more consistent with the acyl complex **7**. In particular, the CO stretching pattern for an Fe$(CO)_3$ unit appears (2012 and 1990 cm^{-1}, strong) along with a broad asymmetric peak of moderate intensity at 1760 cm^{-1}.

(16) In **2**, the alkylidene carbon signal appears at δ 326.0.

Relationship between Aromatic Character and Hydrogen Chain Systems

R. C. Haddon,* Krishnan Raghavachari, and M. H. Whangbo†

AT&T Bell Laboratories
Murray Hill, New Jersey 07974

Received January 27, 1984

In a recent publication on the stability of polygonal H_N hydrogen chain systems (HCS),[1] Ichikawa[2] has proposed that these structures may be used as models for Hückel (HMO) aromatic character in the annulenes. We have previously examined this scheme, and the present communication points out the difficulties inherent in such an approach.

The use of hydrogen atoms to model π-electron systems is attractive for two reasons: (i) the two problems give rise to molecular orbitals of the same topological symmetry; (ii) it is possible to model the π-electron system without complications arising from the rigid stereochemistry of the σ-bonds present in organic molecules. In this way, for example, it is possible to make a straightforward comparison of the resonance energies in the [10]annulene, naphthalene, and azulene frameworks by simply

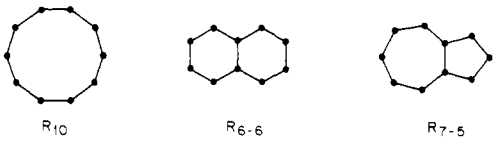

replacing the C or CH groups with hydrogen atoms at an appropriate internuclear separation. Such an energy difference reflects the differing topologies of the systems without the necessity of a correction for angle strain.

The problem with this approach to topological resonance energies resides in a basic incompatability between HCS and HMO aromatic character which may be made transparent from a consideration of delocalization (DE) and resonance (RE) energies.[3-15] In keeping with the HMO practice of assigning a

† Department of Chemistry, North Carolina State University, Raleigh, NC 27650.

(1) Seel, M.; Bagus, P. S.; Ladik, J. *J. Chem. Phys.* **1982**, *77*, 3123 and references therein.

(2) Ichikawa, H. *J. Am. Chem. Soc.* **1983**, *105*, 7467.

(3) The DE is defined in the present context as the calculated additional bonding energy that results from delocalization of electrons originally constrained to isolated double bonds (HMO)/hydrogen molecules (HCS). Streitwieser, A. "Molecular Orbital Theory for Organic Chemists"; Wiley: New York, 1961; Chapter 9.

(4) Both the DE and RE are considered on a per electron (PE) basis for comparison purposes. Positive values (in units of positive β for HMO systems) denote stabilization.

0002-7863/84/1506-5364$01.50/0

Table I. Calculated Delocalization and Resonance Energies per Electron for the HMO and HCS Schemes

topological structure[a]	HCS,[b] kcal/mol				HMO (β) REPE						Dewar[7] REPE (SCF/MO), kcal/mol
	DEPE[c]		REPE[c]								
	HF	MP4	HF	MP4	E	DEPE	A-I[10]	A-II, GMT[11]	HS[12,13]	UT[14,d]	
L_2	0.0	0.0			2.0	0.0					
L_4	−17.1	−15.3			4.47	0.118			0.002		
R_4^T	−55.2	−53.5	−31.1	−32.8	4.0	0.0	−0.273	−0.307	−0.268	−0.206	−5.2
R_6	−20.6	−18.8	3.6	1.9	8.0	0.333	0.060	0.046	0.065	0.061	3.7
R_8^T	−34.2	−32.0	−10.0	−11.2	9.66	0.207	−0.066	−0.074	−0.060	−0.062	−0.4
R_{10}	−21.6	−19.3	2.6	1.5	12.94	0.294	0.021	0.016	0.026	0.021	1.0
R_{6-6}	−26.7	−24.1	−2.5	−3.4	13.68	0.368		0.039	0.055		3.4
R_{7-5}	−32.2	−29.3	−8.0	−8.6	13.36	0.336		0.015	0.023		0.7

[a] L and R signify linear and ring (regular polygonal) structures, respectively. The subscripts refer to the number of centers involved in conjugation. The triplet states of R_4 and R_8 were only employed in the HF and MP4 calculations. [b] HF/STO-6G structures and energies for R_6 and R_{10} were taken from ref 2. Structural optimizations of L_4, R_{6-6}, and R_{7-5} were carried out with a single common H–H bond length. The bond lengths and HF and MP4 energies per electron were obtained: L_2, 0.7105 Å, −0.56311 hartree, −0.57239 hartree; L_4, 0.8511, −0.53585, −0.54802; R_4^B, 1.1437, −0.44996, −0.48079; R_4^C, 1.1165, −0.43157, −0.44343; R_4^T, 1.1469, −0.47511, −0.48710; R_6, 0.9553, −0.53035, −0.54238; R_8^B, 1.0061, −0.50363, −0.52089; R_8^C, 0.9993, −0.49961, −0.51088; R_8^T, 1.0045, −0.50861, −0.52141; R_{10}, 0.9455, −0.52872, −0.54170; R_{6-6}, 1.0049, −0.52062, −0.53391; R_{7-5}, 1.0090, −0.51184, −0.52567; R_{26}, 0.9409, −0.52548, −0.53978; R_{30}, 0.9408, −0.52524, −0.53965; R_{34}, 0.9407, −0.52507, −0.53956; R_{38}, 0.9407, −0.52495, −0.53949; R_∞, 0.9407 ± 0.0002, −0.5246 ± 0.0002, −0.5393 ± 0.0002. [c] Calculated from the formulas $DEPE(X_n) = -[E^{PE}(X_n) - E^{PE}(L_2)]$ and $REPE(X_n) = -[E^{PE}(X_n) - E^{PE}(R_\infty)]$, where $E^{PE}(X_n)$ denotes the total energy per electron for a given n electron ring (X = R) or linear (X = L) structure. [d] Unified Theory.[14] Resonance energies for the antiaromatic rings were obtained from the formulas $RE = -2\pi^2 p_{rs}\beta/(3N) = -\pi^2 E/(3N^2) = -4\pi^2\beta/[3N^2 \tan(\pi/N)]$ (cf. eq 25, ref 14). Thus the resonance destabilization (antiaromaticity) of these systems is approximately double the stabilization of their aromatic counterparts for a "given value of N". Haddon, R. C., unpublished results.

common resonance integral (β) to all π-bonds, the HCS Hartree–Fock (HF) geometry optimizations were carried out with a common nearest-neighbor H–H bond distance and the rings (R) were constrained to be regular polygons and the chains to be linear (L). The STO-6G[16] basis set, which was employed in the previous publication on HCS,[2] has been adopted throughout this study. Consider first the DE in HMO butadiene and HF HCS linear H_4 as given by

(1)

The energies are DEPE(HMO) = 0.118β and DEPE(HCS) = −17.1 kcal/mol. Thus in the HMO approach the DE across the partial π-bond is stabilizing whereas the HCS is destabilized by this interaction. The DEs for the HMO and HCS analyses are summarized in Table I—the *sign* of this quantity in the two schemes is seen to disagree throughout.

If eq 1 is rewritten as an isodesmic reaction, allowing contact with real chemistry the conjugation energy is obtained as 14.2 (expt), 12.3 (STO-3G), and 11.2 (4-31G)[5] kcal/mol, again sug-

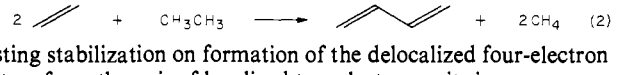

(2)

gesting stabilization on formation of the delocalized four-electron system from the pair of localized two-electron units in consonance with the HMO result.

Modern systems of aromatic character follow Dewar[6-8] in redefining the nonaromatic reference structure which may be taken from the conjugated single and double bonds in a finite or infinite linear polyene. Within this approach the annulenes were found to possess a wide and continuous spectrum of resonance energies, which included both positive (aromatic) and negative (antiaromatic) values.[6-9] The results of such an analysis of HCS based on the "infinite" hydrogen ring reference structure (R_∞) are contrasted with modern theories of the resonance energy[6-15] in Table I. The R_∞ structure and energies were obtained by geometric extrapolation of the results obtained for R_{26}, R_{30}, R_{34}, and R_{38}. It is clear that the parallels in the computed REs for the HMO and HCS are superficial at best. For the aromatic rings the REs in the HCS analysis are very small, and the largest deviation from the reference energy is provided by the small antiaromatic rings. However, the treatment of these systems with restricted HF techniques must be regarded as suspect because of the first-order Jahn–Teller instability (e^2) exhibited by the wave function which is of lower symmetry than the nuclear framework.

Within the HF approximation for H_N rings and [N]annulenes at D_{Nh} symmetry there are two possible singlet states corresponding to the bond density wave (BDW) and charge density wave (CDW) broken symmetry solutions.[17] The highest occupied molecular orbital for the two cases in the four-membered ring is shown below.

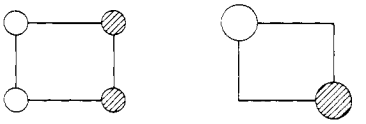

The previously reported[2] structures and energies of H_4 and H_8 correspond to the CDW solution, which we find to be higher in energy than the BDW cases. For the antiaromatic rings, the triplet states represent the only well-defined HF solution, and these results are presented in the body of Table I with the other solutions included as footnotes.

The use of the HCS treatment to obtain topological REs of condensed systems is also seen to be unworkable. The HMO π-electron results in Table I show that REs decrease in the order naphthalene > azulene ~ [10]annulene, whereas the HCS analysis gives [10]annulene > naphthalene > azulene. All are found to be aromatic with the HMO methodology, but both naphthalene and azulene turn out to be antiaromatic with the HCS approach. The modern HMO and SCF/MO RE schemes have been shown to provide an excellent description of the properties of conjugated organic molecules.[6-15]

The inclusion of electron correlation (full MP4)[18] in the calculations has very little effect on the results. The largest changes occur for the REs of R_6 and R_{10}, which are significantly reduced by preferential stabilization of the R_∞ reference structure.

(5) Haddon, R. C.; Starnes, W. H. *Adv. Chem. Ser.* **1978**, *169*, 333.
(6) Dewar, M. J. S. *Adv. Chem. Phys.* **1965**, *8*, 65.
(7) Dewar, M. J. S. *Spec. Publ.—Chem. Soc.* **1967**, *No. 21*, 177.
(8) Dewar, M. J. S.; de Llano, C. *J. Am. Chem. Soc.* **1969**, *91*, 789.
(9) Breslow, R. *Chem. Eng. News* **1965**, *43* (*June 28*), 90.
(10) Aihara, J. *J. Am. Chem. Soc.* **1976**, *98*, 2750.
(11) Gutman, I.; Milun, M.; Trinajstic, N. *J. Am. Chem. Soc.* **1977**, *99*, 1692.
(12) Hess, B. A.; Schaad, L. J. *J. Am. Chem. Soc.* **1971**, *93*, 305.
(13) Hess, B. A.; Schaad, L. J. *Tetrahedron Lett.* **1972**, 5113.
(14) Haddon, R. C. *J. Am. Chem. Soc.* **1979**, *101*, 1722.
(15) Herndon, W. C. *J. Am. Chem. Soc.* **1973**, *95*, 2404.
(16) Hehre, W. J.; Ditchfield, R.; Stewart, R. F.; Pople, J. A. *J. Chem. Phys.* **1970**, *52*, 2769.
(17) Whangbo, M.-H. *Acc. Chem. Res.* **1983**, *16*, 95 and references therein.
(18) Krishnan, R.; Frisch, M. J.; Pople, J. A. *J. Chem. Phys.* **1980**, *72*, 4244.

There is little parallel between the HMO and HCS analysis of aromatic character.[19,20] Perhaps in restrospect this is to be expected but an intriguing question remains: why does HMO theory reflect so accurately the realities of conjugation in organic π-electron systems?

(19) The possibility remains that this type of analysis would succeed with other elements such as lithium where the bond strength between pairs of atoms is weaker than it is in hydrogen. The overwhelming stability of diatomic hydrogen in comparison to extended structures is a primary problem in the HCS analysis. The ability of lithium to form a metal contrasts with the molecular solid formed in the solid state by hydrogen (at atmospheric pressure).

(20) The results also throw some doubt on the practice of modeling conjugated organic polymers with HCS.

Carbene Insertion into Methanol: A Case of Reversible Ylide Formation

Philip M. Warner* and I-Shan Chu

Department of Chemistry, Iowa State University
Ames, Iowa 50011

Received May 29, 1984

We[1] recently demonstrated that the Skattebol rearrangement[2] of **3** (to **4**)[3] proceeds via free carbenes. To gain insight into the mechanism(s) by which these carbenes insert into MeOH, we investigated the solvent deuterium isotope effects for the reaction shown in Scheme I.

Three general mechanisms for the insertion of **3** and **4** into MeOH may be considered: (1) initial protonation to give a carbocation[4] (e.g., eq 1), (2) possibly reversible[4a,5] ylide formation

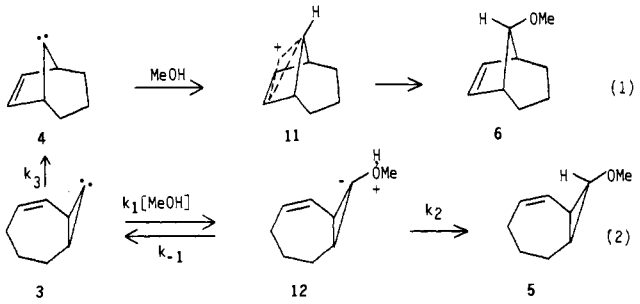

(e.g., eq 2), and (3) direct, three-center, O–H bond insertion. Table I summarizes the isotope effect data we have obtained at room temperature. The percent deuterium incorporations were obtained by GC-Ms at low-ionizing voltages.[6] Despite some scatter, the isotope effects are not a function of the [MeOH].[7] Table II displays the temperature-dependent isotope effects, measured in 20% methanolic benzene (or toluene). Rearranged product **6** shows a consistently secondary isotope effect, with small differential activation parameters ($\Delta\Delta H^{\ddagger} \approx 50$ cal/mol, $\Delta\Delta S^{\ddagger} \approx 0$). This is consistent with a constant mechanism over the temperature range studied. Although a secondary isotope effect might be unexpected for either the protonation (eq 1) or direct insertion mechanisms, it is appropriate for eq 1 if the reaction is close to diffusion controlled.

The dramatically different isotope effect seen for **5** at −78 °C is explicable by a change in the rate-determining step with temperature. Thus the first step in eq 2 is rate limiting at the higher temperatures (secondary isotope effect), while the proton-shift step[8] becomes the slow one at low temperature (primary isotope

Scheme I

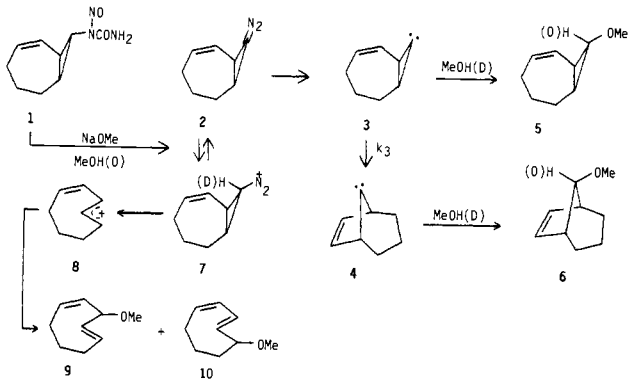

Table I. Room Temperature Solvent Isotope Effect Data[a,b]

conditions	k_H/k_D[e] 5	k_H/k_D[e] 6
30% methanol[c]	1.15	1.17
50% methanol[c]	1.41	1.10
80% methanol[c]	1.15	1.08
100% methanol[c]	1.33	1.23
MeOH:MeOD = 1:2 (v/v)[d]	1.13	1.19
MeOH:MeOD = 1:1 (v/v)[d]	1.15	1.08
MeOH:MeOD = 2:1 (v/v)[d]	1.06	0.93

[a] All reactions were carried out at [1] = 0.051 M, [NaOMe] = 0.185 M, and with benzene as the cosolvent. [b] Deuterium incorporations in 80% MeOD/20% PhH were **5**, 98.3%; **6**, 99.9%. [c] MeOH:MeOD = 1:1 (v/v). [d] Total methanol = 80%. [e] The error is difficult to estimate, but from duplicate runs, ± 0.05 to ± 0.15 seems reasonable.

Table II. Variable-Temperature Solvent Isotope Effects

temp, °C	k_H/k_D 5	k_H/k_D 6
40[a]	1.06	0.96
24[a]	1.15	1.01
10[a]	1.20	1.02
−78[b,d]	2.21	1.10
−78[c,d]	2.85	1.25

[a] Reactions in 40% MeOH/40% MeOD/20% benzene (by volume), with [1] = 0.051 M and [NaOMe] = 0.185 M. [b] Reaction in 40% MeOH/40% MeOD/20% toluene with same [1] and [NaOMe] as at high temperatures. [c] Same as *b*, but with MeOH:MeOD = 1:2. [d] Deuterium incorporations in 80% MeOD/20% toluene were **5**, 94.5%; **6**, 99.2%. This may indicate a small amount of **5** arises from unexchanged **7** at −78 °C.

Table III. Activation Parameters Based on **6**/**5** Ratios[a]

R[slope(high T)] = $\Delta H_1^{\ddagger} - \Delta H_3^{\ddagger}$ = −4.9 ± 0.3 kcal/mol
$-R$[intercept(high T)] = $\Delta S_1^{\ddagger} - \Delta S_3^{\ddagger}$ = −26 ± 1 eu
R[slope(low T) − slope(high T)] = $\Delta H_2^{\ddagger} - \Delta H_{-1}^{\ddagger}$ = 3.7–4.9 kcal/mol
$-R$[intercept(low T) − intercept(high T)] = $\Delta S_2^{\ddagger} - \Delta S_{-1}^{\ddagger}$ = 13–19 eu

[a] Data is corrected for k_H/k_D differences.

(1) Warner, P.; Chu, I-S. *J. Org. Chem.*, accepted for publication.
(2) Skattebol, L. *Tetrahedron* **1967**, *23*, 1107.
(3) Kirmse, W.; Richarz, U. *Chem. Ber.* **1978**, *111*, 1883.
(4) (a) Kirmse, W.; Loosen, K.; Sluma, H.-D. *J. Am. Chem. Soc.* **1981**, *103*, 5935. (b) Kirmse, W.; Van Chiem, P.; Henning, P. G. *Ibid.* **1983**, *105*, 1695.
(5) Bethell, D.; Newall, A. R.; Wittaker, D. *J. Chem. Soc. B* **1971**, *23*.
(6) Isotope effects for **9** and **10** were difficult to determine accurately due to (a) incorporation of only ca. 82% *d* in **9** and 86% *d* in **10** in 80% MeOD/20% PhH and (b) large P-1 and P-2 peaks in the mass spectra. The values obtained at room temperature were k_H/k_D(**9**) = 1.9, k_H/k_D(**10**) = 2.9; at −78 °C they were k_H/k_D(**9**) = 2.5, k_H/k_D(**10**) = 3.4. We do not yet know if these values are really different.
(7) (a) MeOH is aggregated over the entire (high) concentration range we examined. Thus one would not expect the nonlinear behavior seen by Griller[7b] at quite low [MeOH] due to different methanol oligomers. (b) Griller, D.; Liu, M. T. H.; Scaiano, J. C. *J. Am. Chem. Soc.* **1982**, *104*, 5549.

0002-7863/84/1506-5366$01.50/0